Pergamon

Bioorganic & Medicinal Chemistry 7 (1999) 1979–1991

BIOORGANIC & MEDICINAL CHEMISTRY

$tRNA^{Phe}$ Binds Aminoglycoside Antibiotics

Sarah R. Kirk and Yitzhak Tor*

Department of Chemistry and Biochemistry, University of California, San Diego, La Jolla, CA 92093-0358, USA

Received 20 January 1999; accepted 14 April 1999

Abstract—Aminoglycoside antibiotics have recently been found to bind to a variety of unrelated RNA molecules, including sequences that are important for retroviral replication. We report the binding of neomycin B, kanamycin A, and Neo–Neo (a synthetic neomycin–neomycin dimer) to $tRNA^{Phe}$. Using thermal denaturation studies, fluorescence spectroscopy, Pb^{2+}-mediated $tRNA^{Phe}$ cleavage, and gel mobility shift assays, we have established that aminoglycosides interact with yeast $tRNA^{Phe}$ and are likely to induce a conformational change. Thermal denaturation studies revealed that aminoglycosides have a substantial stabilizing effect on $tRNA^{Phe}$ secondary and tertiary structures, much greater than the stabilization effect of spermine, an unstructured polyamine. Aminoglycoside-induced inhibition of Pb^{2+}-mediated $tRNA^{Phe}$ cleavage yielded IC_{50} values of: 5 μM for Neo–Neo, 100 μM for neomycin B, >1 mM for kanamycin A, and >10 mM for spermine. Enzymatic and chemical footprinting indicate that the anticodon stem as well as the junction of the TψC and D loops are preferred aminoglycoside binding sites.

Introduction

RNA molecules are functionally sophisticated and play key roles in essential biological processes such as protein biosynthesis, transcriptional regulation, and retroviral replication. This functional diversity is intimately associated with the ability of RNA sequences to form complex three-dimensional structures. These intricate folds project multiple functional groups capable of both binding other biomolecules and generating potential binding pockets for metal ions and small molecules. Consequently, RNA molecules are attractive targets for therapeutic intervention.[1,2] The design of small molecular effectors that specifically target RNA presents, however, an unusual challenge that requires an intimate knowledge of RNA structure, folding, and recognition. Currently, designing specific RNA binders is an empirical task and fundamental aspects of RNA–small molecule recognition remain elusive.[3]

Aminoglycoside antibiotics, a family of polycationic pseudo-oligosaccharides, have recently emerged as an intriguing family of RNA binders.[3] These highly charged molecules contain a 2-deoxystreptamine core that is typically glycosylated at either the four and five hydroxyls or the four and six hydroxyls with amino sugars (see Fig. 1). Their well-established interference with protein biosynthesis via their specific binding to prokaryotic 16S ribosomal RNA[4] triggered an extensive search for other potential RNA targets. Aminoglycosides have since been shown to bind and inhibit the self-splicing of group I introns,[5–7] the hammerhead ribozyme,[8,9] and hepatitis delta virus ribozyme.[10,11] They have also been shown to block the binding of the Rev protein[12] and the Tat peptide[13] to their viral RNA targets. While it appears that these antibiotics interact with seemingly unrelated RNA targets, it is likely that they recognize similar structural motifs within the folded RNA structures. Electrostatic interactions have been demonstrated to be critical in RNA–aminoglycoside binding,[9] and a dynamic recognition model emphasizing structural electrostatic complementarity has been proposed.[14–16] In vitro selection experiments[17–19] and high resolution NMR studies[20–23] have begun to reveal the elements involved in RNA–aminoglycoside binding.

While aminoglycoside antibiotics provide a useful lead for the design of new RNA binders,[3] their promiscuous binding to numerous RNA targets raises concerns regarding their binding specificity.[24–26] Since RNA recognition is likely to be 'shape-specific' rather than sequence-specific, multiple targets for a given binder may coexist. High concentration of competing RNA targets might therefore result in scavenging of the binder. Approximately 80–85% of the total cellular RNA is present as rRNA, while 10–15% is tRNA, and the remaining 2–5% is mRNA.[27] Since mRNA is rather

Key words: Aminoglycoside antibiotics; tRNA; RNA recognition; small molecules.

* Corresponding author. Tel. +1-858-534-6401; fax: +1-858-534-5383; e-mail: ytor@ucsd.edu

0968-0896/99/$ - see front matter
PII: S0968-0896(99)00170-4

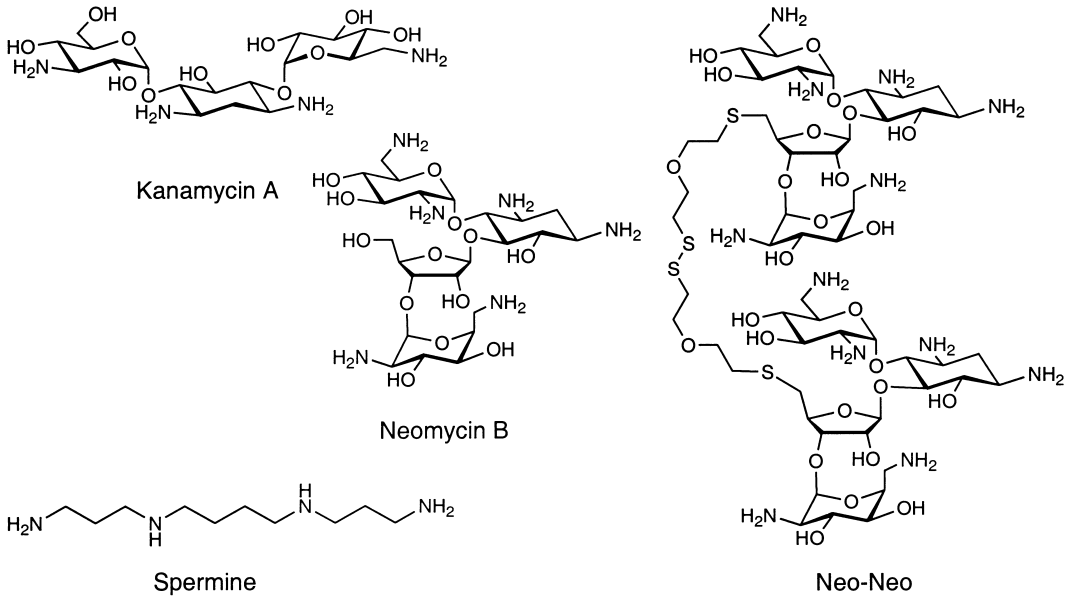

Figure 1. Structure of natural aminoglycoside antibiotics (kanamycin A, neomycin B), a synthetic aminoglycoside dimer (Neo–Neo) and an unstructured polyamine (spermine).

short-lived and rRNA is complexed to ribosomal proteins, tRNA comprises the majority of the soluble cytoplasmic RNA. Therefore, it is critically important to evaluate whether tRNA can bind aminoglycoside antibiotics.

To shed light on the interactions between aminoglycoside antibiotics and tRNA, we examine the binding of natural and synthetic aminoglycosides to phenylalanine-specific tRNA ($tRNA^{Phe}$). $tRNA^{Phe}$ is one of the most thoroughly studied natural RNA molecules.[28,29] Its three-dimensional structure has been revealed by high-resolution X-ray crystallography,[30] and its solution properties have been characterized by numerous biophysical techniques.[31] The three dimensional structure of $tRNA^{Phe}$ encompasses many structural motifs. Due to well-defined tertiary interactions (Fig. 2), folded $tRNA^{Phe}$ contains several distinct environments that can serve as binding sites for small molecules. The binding of Mg^{2+} and other metal ions has been extensively studied, and binding sites for the polycationic spermine have been revealed.[28,32–36] The similarity in folding patterns of most tRNA molecules makes $tRNA^{Phe}$ a valuable natural biopolymer for investigating RNA–small molecule recognition.

Figure 1 shows the aminoglycosides studied: neomycin B, kanamycin A, and neomycin–neomycin dimer (Neo–Neo). Kanamycin A has four amino groups and is a strong inhibitor of translation and a weak inhibitor of self-splicing.[5] Neomycin B contains six amino groups which are predominantly protonated at physiological pH,[37] and is among the strongest inhibitors of in vitro translation and group I intron self-splicing.[5] Neo–Neo, a synthetic dimer of neomycin B containing 12 amino groups, was designed to be a potent RNA binder with a high number of positive charges and potential binding to multiple sites.[38] Neo–Neo was found to be approximately sixfold more effective at inhibiting the self-splicing of the

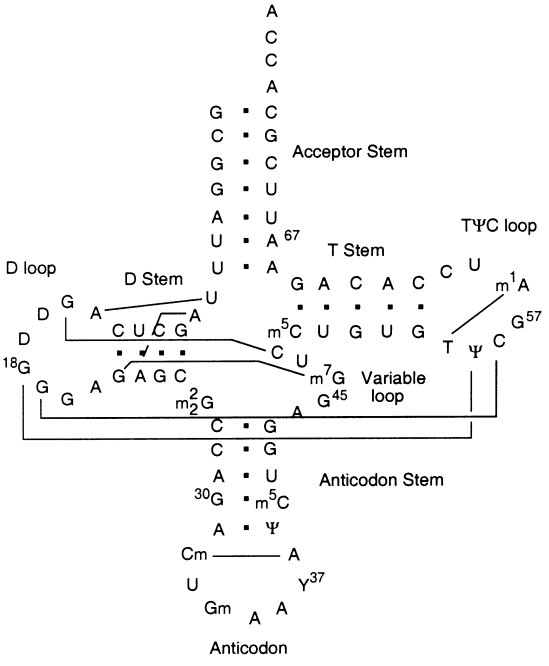

Figure 2. Sequence and secondary structure of $tRNA^{Phe}$. Base pairing is indicated by dots, and lines indicate tertiary interactions formed upon proper folding.

hammerhead ribozyme,[38] and about 20-fold more effective at inhibiting the self-splicing of the *Tetrahymena* ribozyme[39] than its monomeric parent compound, neomycin B. Spermine was included in this study because it is a non-aminoglycoside simple polyamine that is known to bind $tRNA^{Phe}$.[32,33,36] With spermine as a control compound, it is possible to assess whether any effects observed in the presence of aminoglycosides are merely due to 'nonspecific' electrostatic interactions or if a significant role is played by the three-dimensional representation of the ammonium groups on the aminoglycosides.

Using thermal denaturation studies, fluorescence spectroscopy, Pb^{2+}-mediated $tRNA^{Phe}$ cleavage, gel mobility shift assays, as well as enzymatic and chemical footprinting, we have established that aminoglycosides interact with yeast $tRNA^{Phe}$ and are likely to induce a conformational change. We propose multiple binding sites for aminoglycosides on $tRNA^{Phe}$ and discuss the implications of this recognition event on the design of RNA binders.

Results

Thermal denaturation studies

Spermine, kanamycin A and Mg^{2+} are individually added to $tRNA^{Phe}$ (0.38 μM) in a 50 mM Tris–HCl buffer (pH 7.0) containing NaCl (100 mM). The change in absorbance of each sample is measured at 260 nm as a function of temperature. Melting temperature (T_m) values are obtained by calculating the first derivative of the resulting melting curves. In the absence of any additives, $tRNA^{Phe}$ shows a broad melting curve with a T_m at 65°C (Fig. 3). Addition of either kanamycin A (1 mM) or Mg^{2+} (2 mM) to $tRNA^{Phe}$ results in a substantial increase in the melting temperature ($\Delta T_m = 10$°C) while the ΔT_m obtained for spermine (1 mM) is only 6°C (Fig. 3(a)). Melting curves measured in the presence of Mg^{2+} are generally much steeper than curves obtained with either spermine or kanamycin A. Upon addition of neomycin B (10 μM) to $tRNA^{Phe}$ (0.38 μM), a ΔT_m of 14°C is determined, with a very steep curve which resembles the curve obtained in the presence of Mg^{2+} (Fig. 3(a)). Neomycin B is by far the most effective ligand for stabilizing $tRNA^{Phe}$ against unfolding.[40] The effect of spermine, kanamycin A, or neomycin B on $tRNA^{Phe}$ stability is also measured in the presence of $MgCl_2$ (1 mM). A slight shift to higher temperatures is observed upon addition of all polyamines (same concentrations as above). In the case of spermine and kanamycin A, steeper curves are observed which resemble the melting curve of $tRNA^{Phe}$ in the presence of Mg^{2+} or neomycin B (Fig. 3(b)).

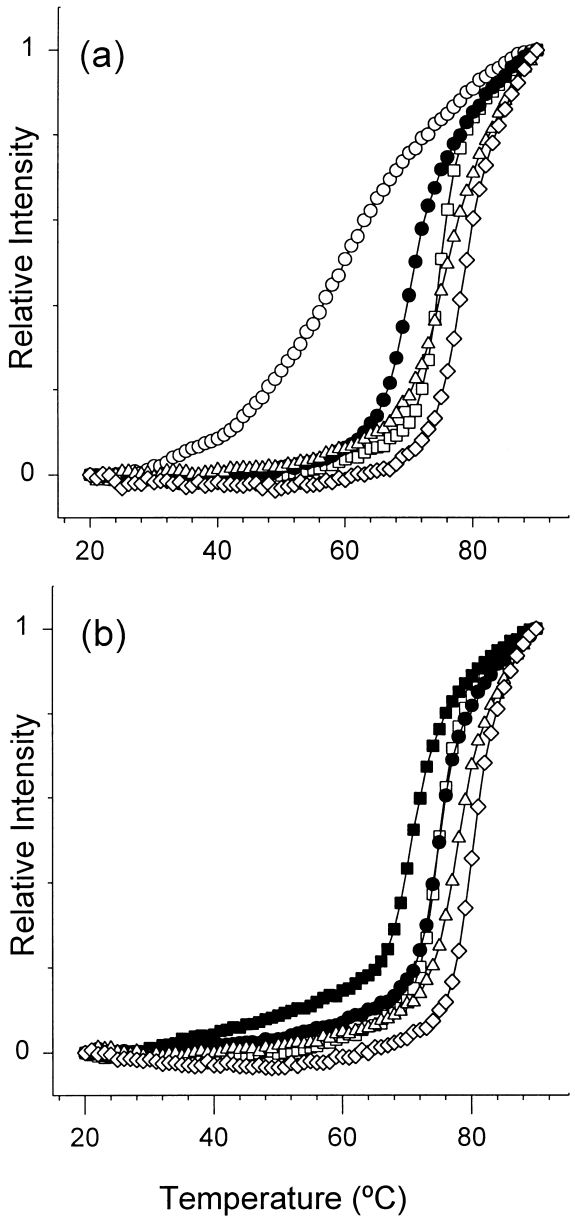

Figure 3. (a) Thermal denaturation curves of 0.38 μM $tRNA^{Phe}$ in the absence (○) and in the presence of: 2 mM $MgCl_2$ (□), 1 mM spermine (●). 1 mM kanamycin A (Δ), and 10 μM neomycin B (◇). (b) Themal denaturation curves of 0.38 μM $tRNA^{Phe}$ in the presence of: 1 mM $MgCl_2$ (■), 1 mM spermine + 1 mM $MgCl_2$ (●), 1 mM kanamycin A + 1 mM $MgCl_2$ (Δ), 2 mM $MgCl_2$ (□), and 10 μM neomycin B + 1 mM $MgCl_2$ (◇).

Fluorescence spectroscopy

The fluorescence spectrum of $tRNA^{Phe}$ in 50 mM Tris–HCl (pH 7.0) is taken upon excitation at 318 nm. The emission of the Y base at 437 nm is enhanced in the presence of increasing concentration of Mg^{2+}, spermine, kanamycin A, neomycin B, and Neo–Neo. When added to $tRNA^{Phe}$ (0.6 μM), either Neo–Neo or Mg^{2+} cause the largest enhancement of Y base fluorescence followed by neomycin B, kanamycin A, and finally spermine (Fig. 4).

In the presence of Mg^{2+}, a 4 nm red-shift in the emission wavelength is observed as the intensity of the Y base is enhanced. This shift is not observed in the presence of the other ligands. The fluorescence enhancement is less steep than in the presence of spermine but the maximum intensity of the Y base in the presence of Mg^{2+} (1 mM) is 2.6-fold higher than in the presence of spermine (1 mM). Neomycin B yields a maximum intensity that is intermediate between those with kanamycin A and Mg^{2+} (Fig. 4). The concentration of ligand needed to double the Y base fluorescence is approximately 0.9 mM for spermine, 0.5 mM for kanamycin A, 90 μM for neomycin B, 5 μM for Neo–Neo, and 45 μM for Mg^{2+}. At saturation either Neo–Neo or Mg^{2+} enhance fluorescence by 3.6 times, neomycin B by 2.5 times while kanamycin A and spermine double initial Y base fluorescence.

When complexed to $tRNA^{Phe}$ (0.2 μM), ethidium bromide (EB) (4 μM) emits at 598 nm upon excitation at 546 nm.

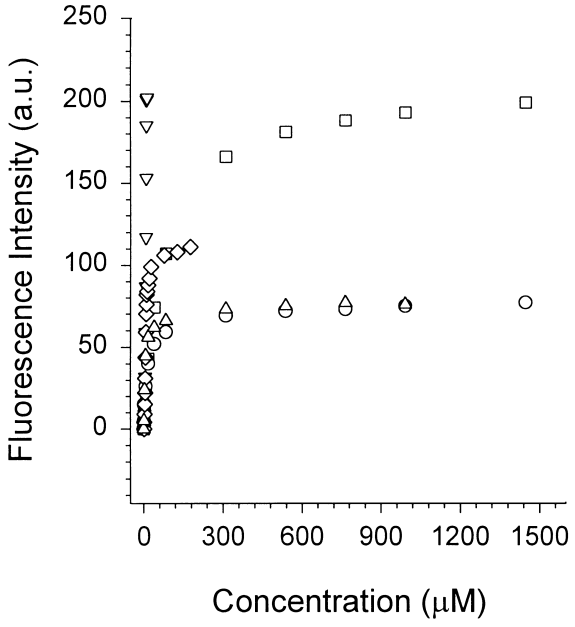

Figure 4. Fluorescence intensity of Y37 of $tRNA^{Phe}$ (0.6 μM) in the presence of increasing concentrations of: spermine (○), kanamycin A (△), neomycin B (◇), Neo–Neo(▽) and $MgCl_2$ (□). The Y base was exited at 318 nm and the emission was monitored at 437 nm.

The emission is diminished upon increasing the concentrations of spermine, Mg^{2+}, and aminoglycosides (Fig. 5). Neomycin B and Neo–Neo decrease fluorescence intensity by about 70% of the initial emission of EB and $tRNA^{Phe}$, while kanamycin B, spermine, and Mg^{2+} decrease EB emission by about 30, 15, and 10%, respectively.[41]

In the presence of Mg^{2+} (1 mM), $tRNA^{Phe}$ solutions containing EB display weaker fluorescence. Upon addition of polyamines, the quenching trend remains the same as described above, but the overall change in fluorescence intensity is smaller. Increasing concentrations of neomycin B, kanamycin A, and spermine diminish fluorescence by >60, 10 and 10%, respectively (Fig. 5). Aminoglycosides or spermine added to a solution of EB in the absence of $tRNA^{Phe}$ do not affect its fluorescence.

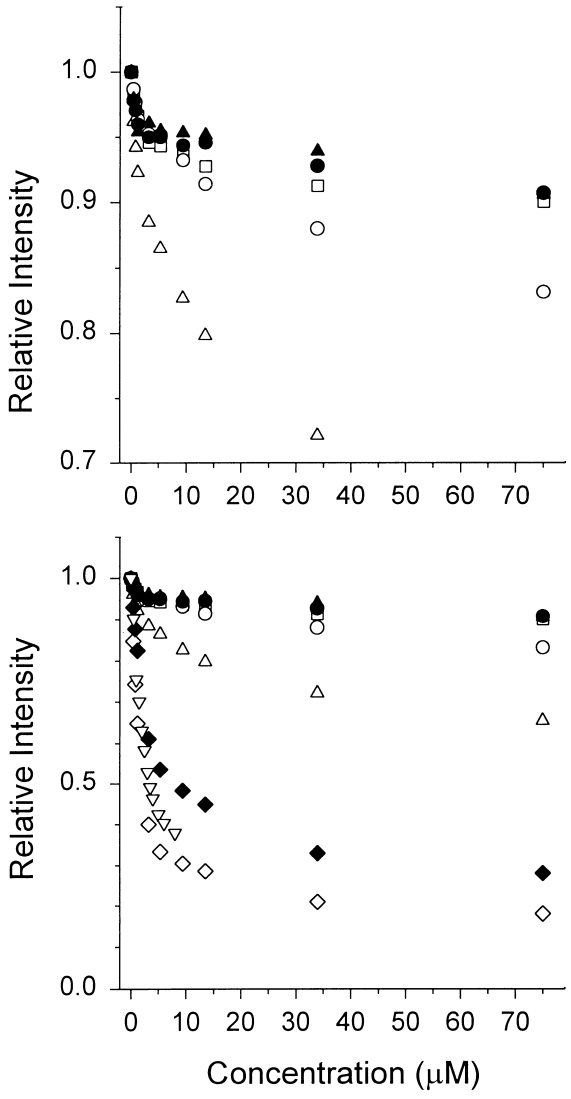

Figure 5. Bottom: Relative fluorescence intensity of ethidium bromide (4 μM) bound to $tRNA^{Phe}$ (0.2 μM) in the presence of increasing concentration of: $MgCl_2$ (□), spermine (○), kanamycin A (△), neomycin B (◇), and Neo–Neo (▽). Relative intensity of ethidium bromide (4 μM) bound to $tRNA^{Phe}$ (0.2 μM) preincubated with $MgCl_2$ (1 mM) and in the presence of: spermine (●), kanamycin A (▲), and neomycin B (◆). The ethidium bromide was exited at 546 nm and the emission was monitored at 598 nm. Top: expansion of bottom graph, same symbols.

Pb^{2+}-mediated $tRNA^{Phe}$ cleavage

Aminoglycoside antibiotics are titrated into a buffered solution of $tRNA^{Phe}$ (2 μM) with traces of 5′- or 3′-labeled $tRNA^{Phe}$ in 50 mM Tris–HCl (pH 7.0) containing $MgCl_2$ (10 mM) and NaCl (100 mM). Aliquots of a $Pb(OAc)_2$ solution (2 mM) are added to a final concentration of 200 μM. The cleavage reaction mixtures are equilibrated for 15 min at room temperature. They are resolved by gel electrophoresis, analyzed, and quantified. As Neo–Neo, neomycin B, kanamycin A and spermine are titrated into the cleavage reaction mixture, the Pb^{2+}-induced cleavage of $tRNA^{Phe}$ diminishes (Fig. 6). Inhibition curves yield IC_{50} values as follows: 5 μM for Neo–Neo, 100 μM for neomycin B, >1 mM for kanamycin A, and >10 mM for spermine.

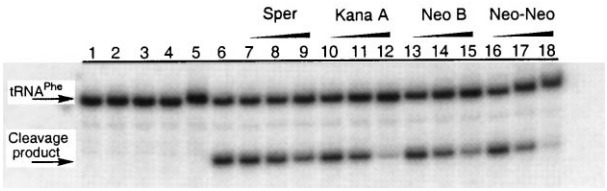

Figure 6. Cleavage of native $tRNA^{Phe}$ by $Pb(OAc)_2$. All lanes contained 2 μM $tRNA^{Phe}$ with trace 3′-^{32}P labeled $tRNA^{Phe}$. Lane 1, control; lane 2, 1 mM spermine; lane 3, 1 mM kanamycin A; lane 4, 100 μM neomycin B; lane 5, 10 μM Neo–Neo. Lanes 6–18 contain 200 μM, $Pb(OAc)_2$, lanes 7–9, 100 μM, 1 mM, 10 mM spermine, respectively; lanes 10–12, 100 μM, 1 mM, 10 mM kanamycin A, respectively; lanes 13–15, 10 μM, 100 μM, 1 mM neomycin B, respectively; lanes 16–18, 1, 10, 100 μM Neo–Neo, respectively.

Gel mobility shift assay

tRNA^{Phe} (2 μM) containing trace 5′-^{32}P tRNA^{Phe} is incubated with increasing concentrations of either Neo–Neo or neomycin B in 50 mM Tris–acetate (pH 6.8), NaCl (20 mM), and $MgCl_2$ (10 mM). The preincubated mixtures are resolved on a native 12% polyacrylamide gel at room temperature (Fig. 7). A mobility shift first appears at 5 μM Neo–Neo (Fig. 7). Fifty percent of tRNA^{Phe} is complexed at approximately 30 μM Neo–Neo. In contrast, no gel shift is observed in the presence of increasing concentrations of neomycin B up to 10 mM (Fig. 7).

Aminoglycoside-induced tRNA^{Phe} cleavage

In the absence of any enzymes or other cleaving agents, strand scission at two sites (Y37 and m^{7}G46) is observed as tRNA^{Phe} is incubated with aminoglycoside antibiotics (Fig. 8). Cleavage at these sites appears at concentrations as low as 1 μM Neo–Neo, 10 μM neomycin B and 1 mM kanamycin A in the presence of 2 μM tRNA^{Phe}. The total amount of cleavage is 1–2% after 1 h at pH 7.0. Kanamycin A displays a slightly greater cleavage intensity at m^{7}G46 over Y37, Neo–Neo follows the opposite trend, and neomycin B yields equal intensity at both cleavage sites. In addition, spermine, a known tRNA^{Phe} binder, at concentrations ranging up to 10 mM,

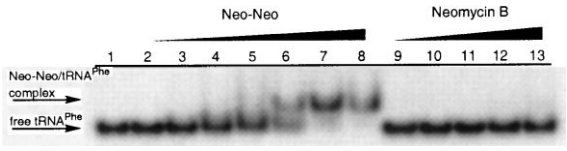

Figure 7. Gel mobility shift of tRNA^{Phe} in the presence of increasing concentrations of Neo–Neo or neomycin B. All lanes contained 2 μM tRNA^{Phe} with trace 5′-^{32}P labeled tRNA^{Phe}. Lane 1, control; lanes 2–8, 1, 5, 10, 15, 30, 50, 100 μM Neo–Neo, respectively; lanes 9–13, 100, 500 μM, 1, 5, 10 mM neomycin B, respectively.

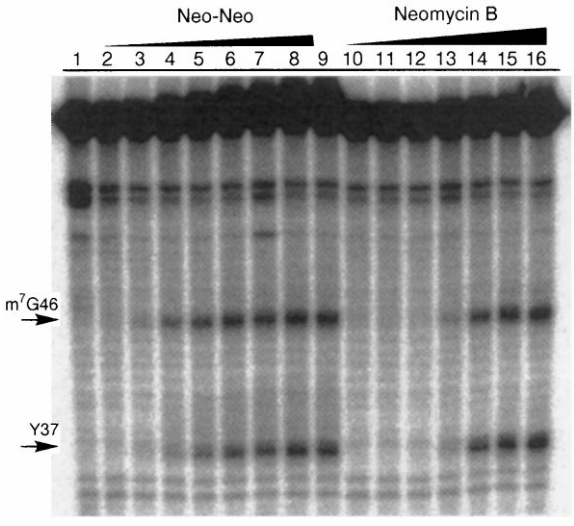

Figure 8. Aminoglycoside-induced cleavage of tRNA^{Phe} at sites Y37 and m^{7}G46. All lanes contained 2 μM tRNA^{Phe} with trace 5′-^{32}P labeled tRNA^{Phe}. Lane 1, control; lanes 2–9, 0.025, 1, 3, 5, 7, 10, 15, 50 μM Neo–Neo, respectively; lanes 10–16, 0.01, 0.1, 1, 10, 100 μM, 1, 10 mM neomycin B, respectively.

shows no cleavage above background at sites Y37 and m^{7}G46. Suppression in cleavage is observed at inherently sensitive sites C28, C56, C61, and C63 (Fig. 8).[42] Aminoglycoside induced hydrolysis of tRNA^{Phe} is observed in all experiments under a variety of conditions.

Enzymatic footprinting

Three ribonucleases are utilized to probe the recognition sites of aminoglycosides on tRNA^{Phe}. RNase T1, which primarily cleaves single stranded RNA at GpN after the 3′ phosphate, reveals protection by aminoglycosides and spermine at nucleotides G18, G19, G20, G30, G42, G43, G51, G53 and G57 (underlining indicates protection to a larger extent; see Figure 9). RNase A cleaves single stranded PypN after the 3′ phosphate. In the presence of aminoglycosides and RNase A, nucleosides C28, U41, ψ55, C56 are identified as sites with major protection while U59, C60, and C61 reveal minor protection by aminoglycosides and spermine. RNase V1 cleaves double stranded regions indiscriminately after the 3′ hydroxyl group. Sites C27, C28, A29, and U41 are protected from cleavage in the presence of aminoglycosides and spermine.

All the aminoglycosides, in addition to spermine, show protection at the same sites but to varying degrees. Neo–Neo offers the greatest protection at bases G20, C27, C28, A29, G30, U41, G42, G43, and G51 with minor protection at bases G18, G19, ψ55, C56, G57, U59, C60 and C61. No protection was observed at G53. Neomycin B and kanamycin A, to a lesser extent, elicit protection at bases G18, G19, G20, C27, C28, G30, G42, G43, G51, G53, ψ55, C56, and G57 as well as inferior protection at bases U33, Gm34, U41, U59, C60, and C61. Spermine offers the greatest protection from cleavage at bases C27, C28, G30, U41, G42, G43, G51, G53, ψ55, and C56 and weaker protection at G18, G19, G20, U33, Gm34, G57, U59, C60, and C61. Footprinting sites are localized in two major regions: the anticodon stem and the junction of the TψC and D loops (Fig. 2).

Fe(II)–EDTA footprinting

Fe(II)–EDTA is a nonspecific cleaving agent used to identify tRNA^{Phe} sites that are accessible to hydroxyl radicals.[43,44] tRNA^{Phe} regions that are protected from cleavage, either due to folding or ligand binding, are observed as footprinting. In the presence of increasing concentrations of Neo–Neo and neomycin B, cleavage at nucleosides A14, G15, U16, G20, A21, G22, A23, m^{5}C40, and G42 is suppressed (Fig. 10), localizing the footprinting sites in the D stem and loop as well as the anticodon stem (Fig. 2).

Discussion

Thermal denaturation studies

Thermal denaturation studies are a useful tool for examining the structural stability of nucleic acids and

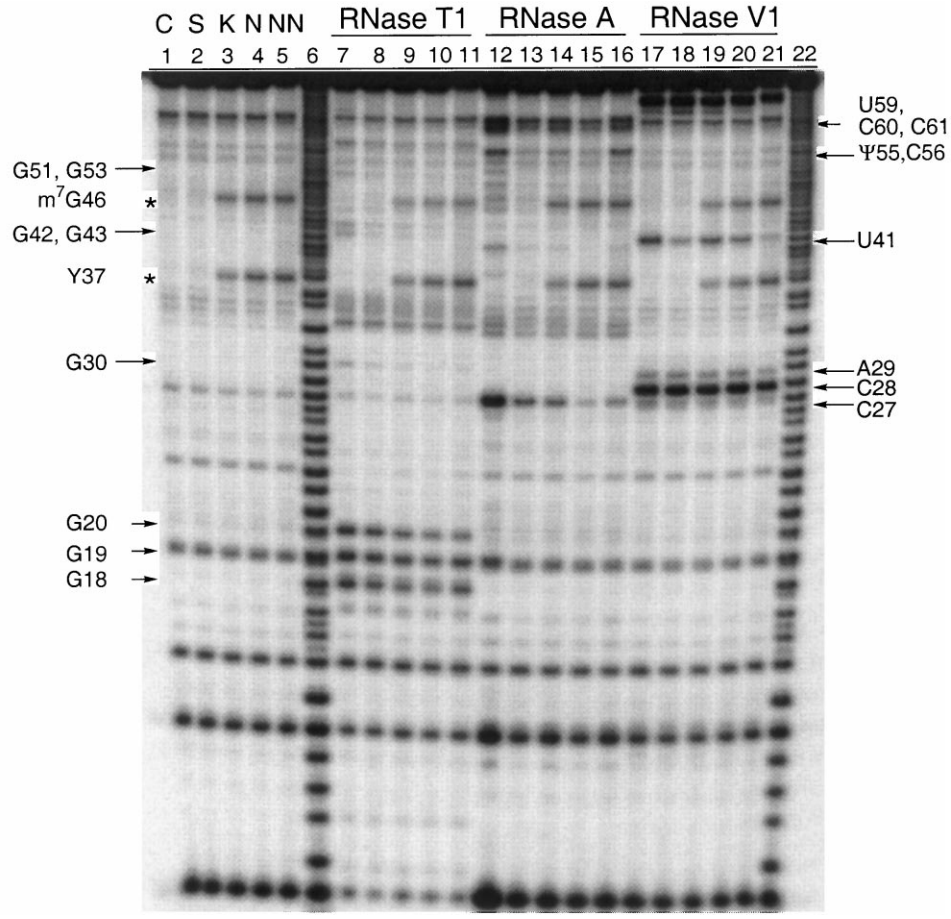

Figure 9. Enzymatic cleavage of $tRNA^{Phe}$ by ribonuclease T1, ribonuclease A, and ribonuclease V1. All lanes contained 2 μM $tRNA^{Phe}$ with trace 5′-^{32}P labeled $tRNA^{Phe}$. Lane 1, control; lane 2, 10 mM spermine; lane 3, 1 mM kanamycin A; lane 4, 100 μM neomycin B; lane 5, 10 μM Neo–Neo; lane 6, base-generated ladder. Lanes 7–11 contain 100 units ribonuclease T1; lane 8, 10 mM spermine; lane 9, 1 mM kanamycin A; lane 10, 100 μM neomycin B; lane 11, 10 μM Neo–Neo. Lanes 12–16 contain 1×10^{-6} units ribonuclease A; lane 13, 10 mM spermine; lane 14, 1 mM kanamycin A; lane 15, 100 μM neomycin B; lane 16, 10 μM Neo–Neo. Lanes 17–21 contain 2.5 units ribonclease V1; lane 18, 10 mM spermine; lane 19, 1 mM kanamycin A; lane 20, 100 μM neomycin B; lane 21, 10 μM Neo–Neo; lane 22, base generated ladder.

other biomolecules. Any change which alters the stability of tRNA is demonstrated by a shift in the heat necessary to denature its complex tertiary and secondary structures. Upon binding of metal ions or other polycationic species to the polyanionic $tRNA^{Phe}$, an increased melting temperature is likely to be observed. Previous studies have shown that, in the presence of Mg^{2+}, melting curves are shifted to higher temperatures.[45] Thermal denaturation studies are therefore employed to measure changes in the structural stability of $tRNA^{Phe}$ in the presence of kanamycin A and neomycin B. Mg^{2+} and spermine (an unstructured polyamine) are utilized as control ligands.

In the absence of polyamines or metal ions, $tRNA^{Phe}$ adopts a rather flexible structure as evidenced by the shallow denaturation curve (Fig. 3). Magnesium ions are essential for the formation of a stable $tRNA^{Phe}$ structure, as illustrated by their important role in the crystallization of $tRNA^{Phe}$.[30] The steeper melting curve obtained in the presence of Mg^{2+} suggest a higher cooperativity of the melting process.[46] In general, upon introduction of each ligand, a shift in the T_m to higher temperatures is observed, suggesting either a greater structural stability of $tRNA^{Phe}$ or a more compact

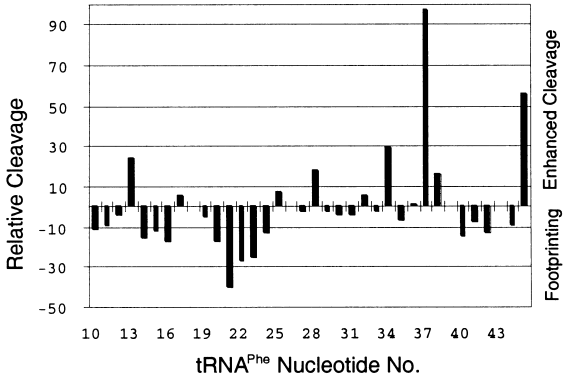

Figure 10. Bar graph indicating normalized footprinting (negative values) and enhanced cleavage (positive values) of $tRNA^{Phe}$ in the presence of Fe(II)–EDTA and Neo–Neo (see Experimental for conditions).

folding. Aminoglycosides are found to be far more effective at stabilizing the three-dimensional folding of $tRNA^{Phe}$ than spermine, with neomycin B having the greatest effect (Fig. 3). These trends cannot be fully explained by exclusively considering the overall charge of the ligands. The three dimensional projection of positive charges by the ligands must also play a role in RNA binding. For example, spermine is more basic than

kanamycin A and is likely to have a greater overall positive charge at physiological pH.[47,48] Yet, kanamycin A stabilizes $tRNA^{Phe}$ to a greater extent than spermine. The higher overall charge of neomycin B as compared to spermine or kanamycin A may result in a tighter binding to $tRNA^{Phe}$ which causes the three-dimensional structure to denature in a cooperative fashion at a higher temperature.

Crystallographic studies have shown that spermine spans phosphate residues of complementary strands in the major groove of the anticodon loop.[32,33] It is likely that aminoglycosides recognize a similar structural motif. Through interactions with the bases or phosphates, aminoglycosides may form bridges between individual strands in the stem region. Such stabilization results in a higher melting temperature.

Aminoglycosides may stabilize tertiary interactions as well as secondary interactions by tightening folding at the junction of the TψC and D loops. Base pairs are formed between G18 and ψ55 as well as G19 and C56 upon folding into the correct tertiary structure (Fig. 2). Spermine has been identified to bind in this region suggesting that this site may be a negatively charged pocket.[36] Upon aminoglycoside binding the interaction between the TψC and D loops may be strengthened. An enhanced interaction between the two loops would lead to a steeper melting curve as observed. It is worth noting that tobramycin, an aminoglycoside similar to kanamycin A, has been shown to bind to a three-residue turn, similar to the TψC loop, of an RNA aptamer.[20,23]

Fluorescence spectroscopy

$tRNA^{Phe}$ contains a fluorescent Y base located near the anticodon stem at position 37.[49] Ligand binding at the anticodon stem or remote sites may induce a conformational change which could alter its photophysical properties. It has previously been shown that fluorescence is enhanced in the presence of Mg^{2+} due to a conformational change that shields the Y base from solvent.[49] Spermine has also been shown to enhance fluorescence of the Y base but to a much lesser extent.[50] Neomycin B or kanamycin A induce fluorescence enhancement that is intermediate between the enhancement caused by spermine and Mg^{2+}. Neo–Neo, when titrated into solution, enhances Y base fluorescence to the same degree as Mg^{2+}. As evident from Figure 4, there is a correlation between the number of potential positive charges and aminoglycoside effectiveness at enhancing fluorescence. Neo–Neo is by far the most effective at enhancing fluorescence followed by neomycin B and kanamycin A.

Fluorescence enhancement can be caused by either direct interaction with the Y base or by distant binding that induces a conformational change. Both can potentially influence the immediate environment of the Y base. Mg^{2+} acts as a point charge and has been shown to directly interact with the Y base.[34] The red-shift in Y base fluorescence in the presence of Mg^{2+} also suggests direct binding. It is therefore not surprising that Mg^{2+} yields the largest effect on fluorescence enhancement. Both spermine and the aminoglycosides have positive charges that are spread out and are likely to interact with a pocket of negative charge density. Given the positions identified for spermine binding[32,33,36] it is likely that spermine and the aminoglycosides bind at a distant region, such as the anticodon stem, and induce a conformational change which affects the Y base environment.[51] The greatest conformational change is induced by Neo–Neo due to its larger size and abundance of positive charge.

EB is known to intercalate into $tRNA^{Phe}$.[52] Upon intercalation, EB's fluorescence is greatly enhanced. It has been determined that approximately ten molecules of EB are bound to a single tRNA molecule, yet only three molecules of EB are bound in sites that facilitate EB fluorescence.[53] A single strong EB binding site is located adjacent to the sixth base pair of the acceptor stem in $tRNA^{Phe}$.[54]

Upon ligand binding, EB fluorescence is diminished (Fig. 5). Neomycin B and Neo–Neo are the best quenchers followed by kanamycin A, spermine, and Mg^{2+}. Kanamycin A behaves similarly to spermine while Neo–Neo and neomycin B are significantly better at diminishing fluorescence. Quenching may be due to direct displacement of EB by the ligand or a ligand-induced structural change that alters EB binding. There appears to be a correlation between the number of potential charges and the ligand's ability to displace EB. However, neomycin B and Neo–Neo both diminish fluorescence intensity to the same extent, suggesting a possible saturation of effective positive charges. The size of a molecule may also play a role in a ligand's ability to displace EB. Although there is never a complete displacement of EB, maximum quenching by neomycin B is much greater than that obtained by Mg^{2+}. Mg^{2+} may competitively remove less specific binders because it is not large enough to fully displace EB. In contrast, neomycin B has an extended array of charges that might not allow for simultaneous binding of both neomycin B and EB.

Pb^{2+}-mediated $tRNA^{Phe}$ cleavage

Aminoglycoside binding to $tRNA^{Phe}$ is further investigated by examining its effect on the Pb^{2+}-mediated cleavage reaction. Pb^{2+} is known to coordinate to the heterocyclic bases of C60 and U59 in the TψC loop of $tRNA^{Phe}$.[34,55,56] Upon folding into the proper tertiary structure, the TψC loop is brought into contact with the D loop, positioning an aquo Pb^{2+} ion in close proximity to the 2′ hydroxyl of nucleotide D17. This activation of the 2′ hydroxyl leads to hydrolysis of the phosphodiester bond between nucleotides D17 and G18.[34,55] The cleavage efficiency has been found to be very sensitive to the structural integrity and folding of $tRNA^{Phe}$, and even slight perturbations of the tertiary structure alter the extent and pattern of the Pb^{2+}-mediated cleavage.[56–58]

There is a correlation between the number of amino groups on the aminoglycosides and inhibition of Pb^{2+}-mediated

$tRNA^{Phe}$ cleavage. For example, Neo–Neo is the best inhibitor of cleavage while kanamycin A is the least effective aminoglycoside (Fig. 6). However, the total positive charge is only one factor in the ability of aminoglycosides to inhibit Pb^{2+}-mediated cleavage. For instance, Neo–Neo is 20 times more effective than neomycin B at inhibiting Pb^{2+}-mediated cleavage even though it has only twice the number of amino groups. In addition, spermine contains the same number of amino groups as kanamycin A, but is tenfold less potent as a Pb^{2+}-mediated cleavage inhibitor (Fig. 6). This indicates that the three-dimensional array of charges, the microscopic pK_as on the individual amino groups, and/or the degree of hydration may be important for aminoglycoside–RNA binding. Since spermine is more basic and thus likely to be more highly charged at physiological pH than kanamycin A, electrostatic recognition and placement of the amino groups must be a key factor in RNA binding of the aminoglycosides.[15,16]

Several possibilities may explain the diminished Pb^{2+}-induced cleavage of $tRNA^{Phe}$ observed in the presence of aminoglycosides. The drugs may: (1) coordinate to the Pb^{2+} ion, (2) competitively bind $tRNA^{Phe}$ and displace Pb^{2+}, or (3) bind at a distant region and disrupt the tertiary structure. In principle, aminoglycosides could chelate Pb^{2+} through their amino alcohol functionalities; however, due to their overall positive charge at neutral pH, it is highly unlikely that aminoglycosides have any substantial affinity for Pb^{2+} under our experimental conditions. Furthermore, experimental evidence shows that aminoglycosides do not inhibit the Pb^{2+}-mediated cleavage of RNA aptamers[59] or human delta virus ribozyme.[10]

Pb^{2+} is known to bind $tRNA^{Phe}$ at three distinct sites: Pb(1)–U59, C60, Pb(2)–G45, and Pb(3)–Y37.[34] In the crystal structure of $tRNA^{Phe}$, Mg^{2+} is shown to bind near the Pb(1) site, the binding site responsible for $tRNA^{Phe}$ cleavage, such that the two metals cannot bind simultaneously.[34,35,57] In solution, Pb^{2+} binding does not appear to be disrupted by the presence of Mg^{2+}. Rather, cleavage is reduced due to the structural rigidity of the $tRNA^{Phe}$ induced at high salt concentrations.[60] Because metal ion binding sites are likely to have high negative charge density, it is probable that the positively charged aminoglycosides also bind at these regions.[16] They can act similarly to Mg^{2+} by competing with Pb^{2+} for a binding site and reducing cleavage through displacement of the Pb^{2+} ion. Spermine, Sm^{3+} and Lu^{3+} have been shown to bind at the Pb(2) site and Mg^{2+} at the Pb(3) site.[34] Aminoglycosides bound in these regions might inhibit the Pb^{2+}-induced cleavage of $tRNA^{Phe}$ by inducing a conformational change that disrupts the proper tertiary structure. Taking into consideration the thermal denaturation studies discussed above and the inhibition of Pb^{2+}-induced cleavage, it is likely that aminoglycosides bind $tRNA^{Phe}$ at the Pb(1) site and displace the Pb^{2+} ion and/or bind at an entirely different region thus inducing a conformational change. Both binding modes may disrupt the tertiary structure and lead to lower Pb^{2+}-induced $tRNA^{Phe}$ cleavage.

Gel mobility shift assay

Analysis of the gel mobility shift assay and the Pb^{2+}-induced cleavage assay indicate that Neo–Neo has the greatest affinity for $tRNA^{Phe}$ among the aminoglycoside derivatives tested. Unlike the other ligands studied, Neo–Neo forms a strong complex with $tRNA^{Phe}$ which remains intact under the conditions utilized for the gel shift assay (Fig. 7). The binding of neomycin B to $tRNA^{Phe}$ may suffer from a high *off*-rate resulting in the formation of a short-lived complex that cannot be observed by a gel mobility shift assay (Fig. 7).[61] Because thermal denaturation studies and the inhibition of Pb^{2+}-mediated cleavage provide evidence that both neomycin B and kanamycin A bind to $tRNA^{Phe}$, we can deduce that Neo–Neo has a much lower dissociation rate when compared to the monomeric aminoglycosides tested.[39]

Aminoglycoside-induced hydrolysis

$tRNA^{Phe}$ hydrolysis has been previously observed at pH 7.5 in a solution containing $MgCl_2$ (10 mM) in the absence of any chemical probes or enzymes.[42] Cleavage occurs between nucleotides U8-A9, C13-A14, C28-A29, Y37-A38, C56-G57, C61-A62, and C63-A64. A metal ion, such as Mg^{2+} or Pb^{2+}, can catalyze hydrolysis under neutral conditions in several ways: (1) it can position water molecules as nucleophiles attacking the phosphodiester bond, (2) it can activate a water molecule to abstract a proton from the ribose 2′-hydroxyl thus increasing its nucleophilicity, or (3) it can directly coordinate to the phosphate group, thereby increasing its electrophilicity. In addition, $tRNA^{Phe}$ has to be flexible enough to allow the phosphodiester group to adopt the proper transition state necessary for hydrolytic cleavage.[42]

'Hypercleavage' is designated as the strand scission observed in the presence of aminoglycosides under a variety of experimental conditions (Fig. 8). The $tRNA^{Phe}$ hypercleavage we observe may be a result of direct participation of the aminoglycosides in the hydrolysis reaction. Alternatively, the aminoglycoside may induce a conformational change, thus facilitating $tRNA^{Phe}$ hydrolysis by an activated water molecule.[62] Spermine's inability to accelerate $tRNA^{Phe}$ hydrolysis suggests that the aminoglycosides' unique structure is essential for RNA cleavage. We have previously demonstrated that neomycin B is capable of hydrolyzing adenylyl (3′–5′)-adenosine to its degradation products.[63] It is plausible that cleavage is induced by direct interaction of the aminoglycosides with regions of the phosphate backbone near binding sites, although other explanations cannot be excluded. Further support for direct participation of the aminoglycosides in $tRNA^{Phe}$ hydrolysis is the location of the hypercleavage sites at regions of higher negative charge density as illustrated by Mg^{2+}, Pb^{2+} and spermine binding at these sites.[34] We observe diminished cleavage at sites C28, C56, C61, and C63, known to be inherently prone to hydrolysis.[36] This is most likely due to the rigidity of $tRNA^{Phe}$ in the presence of aminoglycosides.

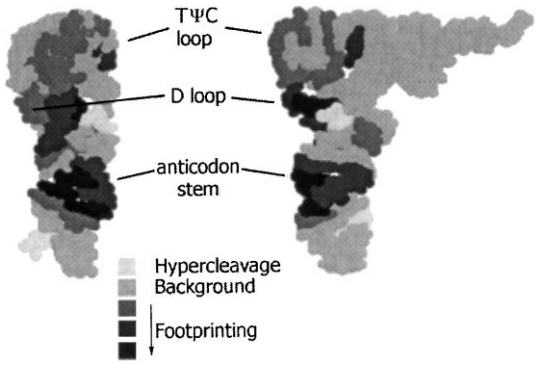

Figure 11. Space-filling model of $tRNA^{Phe}$ (orthographic projection) illustrating hypercleavage sites (light gray) as well as strong (black), medium (dark gray), and weak (gray) protection of nucleotides from enzymatic and chemical cleavage. Figure generated on RasMol using a $tRNA^{Phe}$ pdb file (1tra).

Protection from enzymatic and chemical cleavage

To identify the aminoglycoside binding site(s), enzymatic protection assays are employed (Fig. 9). Nucleotides protected from enzymatic cleavage are grouped into two major regions: nucleotides 27–30 and 41–43, located in the anticodon stem, and nucleotides 18–20 and 51–61, located at the junction of the TψC and D loops (Fig. 11). This suggests that aminoglycoside binding is taking place at double stranded regions next to the anticodon and D loops.

Fe(II)–EDTA cleaves $tRNA^{Phe}$ through the employment of hydroxyl radicals with little or no sequence specificity. $tRNA^{Phe}$ cleavage in the presence of aminoglycosides leads to footprinting at nucleotides A14, G15, U16, G20, A21, G22, A23 located in the D loop and stem regions and m^5C40 and G42 located in the anticodon stem (Fig. 11). Spermine, included in these studies as a control, binds to the major groove of the anticodon stem on $tRNA^{Phe}$ as established by X-ray crystallography[32] and the junction of TψC and D loops as established by NMR spectroscopy.[36]

Aminoglycosides have been shown to bind predominantly in the major groove of RNA.[64] There has been only one reported example of possible minor groove binding.[65] It has also been shown that neomycin B, spermine, and $Co(NH_3)_6^{3+}$ can effectively convert B-DNA to A-DNA.[66] The RNA duplex regions are similar to A-form DNA which has a wide major groove that is associated with a much higher negative potential than the minor groove.[67,68] Due to the polycationic nature of the aminoglycosides, it is anticipated that they bind in the major grooves of $tRNA^{Phe}$ and neutralize the negatively charged surfaces created by the RNA fold.[64]

The major groove of the D stem extending down into the anticodon stem has been recognized as a negatively charged pocket suitable for aminoglycoside binding.[69] In addition, the aminoglycosides are likely to have a flexible conformation and dynamic binding[15] which may lead to footprinting in various positions. Although the enzymatic and chemical footprinting results differ slightly, it is conceivable that some of the protection sites observed may be indirect and result from a rigidity of the molecule due to a big 'counterion' binding. Fe(II)–EDTA and the RNases have distinct modes of cleavage that could lead to footprinting at different sites.

The inhibition of Pb^{2+}-meditated cleavage supports binding in the TψC and D loop. Important contacts are made in the tertiary structure between bases G18-ψ55 and G19-C56. The fidelity of their base pairing is essential for efficient Pb^{2+}-induced cleavage.[57] Protection from enzymatic and chemical cleavage in these regions indicate that aminoglycoside binding is likely to perturb the tertiary structure of $tRNA^{Phe}$. This perturbation of the three dimensional folding reduces Pb^{2+}-mediated cleavage. Notably, a hairpin loop, similar to both the anticodon and the TψC loops, has been identified as a tobramycin binding site on an RNA aptamer.[20,23]

In addition, minor protection from ribonucleases is observed at bases U59, C60, and C61, indicating that direct displacement of Pb^{2+} by aminoglycosides may also occur. Both the change in fluorescence and the location of the hypercleavage site at the Y base suggest that aminoglycosides bind at or near the anticodon stem. The shift in the melting curves also provides support for 'non-covalent cross-linking' of the duplex regions, as well as stabilization of the tertiary interactions. The enzymatic and chemical footprinting results, combined with the other reported studies, suggest that aminoglycosides recognize the $tRNA^{Phe}$ double stranded and distorted loop regions. The anticodon stem as well as the junction of TψC and D loop appear to be the preferred recognition sites (Fig. 11).

Spermine has 3–4 binding sites in yeast $tRNA^{Phe}$ as established by X-ray crystallography and equilibrium dialysis.[32] Intramolecular contacts have been observed at the junction of the TψC and D loop through NMR studies,[36] and the anticodon stem and D stem extending into the variable loop (9–11, 45–47), as seen in crystallography studies.[32] Kanamycin A is likely to bind more strongly at the anticodon stem than at the junction of the TψC and D loops. This is suggested by its larger relative effect on increasing Y base fluorescence than on Pb^{2+}-mediated $tRNA^{Phe}$ cleavage. Additionally, the presence of a hypercleavage site at m^7G46 suggests a possible third binding site at the D stem.

Neomycin B appears to have a comparable affinity for the anticodon stem and the junction of the TψC and D loops. IC_{50} values for Pb^{2+}-mediated $tRNA^{Phe}$ cleavage (100 μM), and the concentration needed to induce a doubling of Y base fluorescence (90 μM) correlate well. Neo–Neo occupies the same sites as neomycin B, but it is unlikely that two neomycin B molecules bind at the site of one dimer. Neo–Neo has a much greater affinity for the anticodon stem, but there is less evidence for tight binding at the junction of the TψC and D loop. The larger size of the dimer may inhibit binding at the second

site. This may occur by either blocking the second site or inducing a structural change that alters the rigidity of the molecule. Although site-selectivity may vary, the aminoglycosides studied seem to bind in the major groove and distorted loop regions of $tRNA^{Phe}$. The three dimensional array of ammonium groups on the aminoglycosides appear to promote binding to sites of high negative charge density on $tRNA^{Phe}$. Since aminoglycosides have an apparent affinity for known metal and spermine binding sites, electrostatic interactions are likely to play a dominant role in aminoglycoside–RNA binding.

Since all known transfer RNA molecules fold into the same cloverleaf secondary structure, the binding of aminoglycosides to $tRNA^{Phe}$ may be a good model for aminoglycoside binding to other tRNAs.[29] The secondary and tertiary structure of tRNA contain diverse structural motifs which can serve as binding sites for small molecules. For small molecules to serve as effective antibacterial and antiviral drugs in vivo, a high affinity and selectivity for a specific RNA site must be achieved. Drugs lacking specificity are likely to be scavenged by tRNA present in the cytoplasm. Our results support the compelling need for the development of potential drugs which bind at specific RNA sites.

Aminoglycoside antibiotics have been shown to bind numerous RNA sequences with little specificity.[24–26] However, it is interesting to note the apparent specificity of aminoglycosides for the rRNA A-site in translational misreading. We speculate that aminoglycosides are capable of simultaneously binding both rRNA and tRNA. The formation of a ternary complex between rRNA, aminoglycoside, and tRNA cannot be excluded. This interaction may constitute an alternative mechanistic explanation for the bactericidal effect of aminoglycoside antibiotics.

Conclusion

Aminoglycoside antibiotics bind to $tRNA^{Phe}$ and are likely to induce a global conformational change. Our data suggest that aminoglycosides bind in double stranded regions adjacent to distorted loops as well as the loops themselves of $tRNA^{Phe}$ and, in particular, the anticodon stem in addition to the junction of TψC and D loops.

Experimental

Materials

Brewers Yeast $tRNA^{Phe}$, spermine (free base), kanamycin $A{\cdot}H_2SO_4$ (containing ca. 5% kanamycin B), and neomycin $B{\cdot}3H_2SO_4$ (containing max 15% neomycin C) were purchased from Sigma. Neomycin $B{\cdot}3H_2SO_4$ and kanamycin $A{\cdot}H_2SO_4$ as well as Neo–Neo[38,39] were converted into their free base form by treatment with Amberlite IRA-400 resin (OH^- form). Stock solutions (10×) of the aminoglycosides were prepared in autoclaved diethyl pyrocarbonate (DEPC) treated H_2O. It was necessary to adjust the pH of aminoglycoside solutions greater than 1 mM with Tris–HCl to ensure pH 7.0. Calf intestinal alkaline phosphatase was purchased from Gibco BRL, dithiothreitol and ribonuclease A from Sigma, bovine serum albumin and ribonuclease T1 from Boehringer Mannheim, adenine triphosphate and ribonuclease V1 from Pharmacia, and T4 polynucleotide kinase and T4 RNA ligase from New England Biolabs. [γ-^{32}P]ATP and [5′-^{32}P]pCp were purchased from NEN®.

Instrumentation

Absorption spectra were taken on a Hewlett–Packard 8452A diode array spectrophotometer. A Varian Cary 1E spectrophotometer with a Cary temperature controller was used for all thermal denaturation studies and a Perkin–Elmer LS50B Luminescence Spectrometer was used for all fluorescence measurements. Gel bands were quantified on a Molecular Dynamics Phosphorimager™ 445 SI and analyzed with Imagequant™ software (Molecular Dynamics).

$tRNA^{Phe}$ labeling

$tRNA^{Phe}$ was dephosphorylated with alkaline phosphatase and 5′-^{32}P labeled with [γ-^{32}P]ATP and T4 polynucleotide kinase.[70] Labeled material was purified by gel electrophoresis on 15% polyacrylamide/7 M urea gels, extracted with 200 mM KOAc, 1 mM EDTA (pH 5.45) for 24 h at 4°C, and ethanol precipitated in the presence of glycogen as a carrier. $tRNA^{Phe}$ was 3′-^{32}P labeled with [5′-^{32}P]pCp and T4 RNA ligase,[71] gel purified and recovered as described above.

Folding of $tRNA^{Phe}$

Solutions of $tRNA^{Phe}$ were heated to 75°C for 3 min and then slowly (1 h) cooled to room temperature before the addition of ligands.

Thermal denaturation studies

$MgCl_2$ (50 μM–2 mM), neomycin B (0.5 μM–100 μM), kanamycin A (15 μM–1 mM) or spermine (15 μM–1 mM) were added to individual tubes of $tRNA^{Phe}$ (0.38 μM) in 50 mM Tris–HCl (pH 7.0) and 100 mM NaCl to a total volume of 1 mL and incubated for 1 h. The concentrations of each ligand were chosen to compensate for the difference in charges. Thermal denaturation curves were determined by following the OD at 260 nm and performed by heating from 20 to 90°C and cooling back to 20°C at 0.5°C/min. T_m values were determined as the maximum of the first derivative of the melting curves.

Fluorescence studies

Solutions of $tRNA^{Phe}$ (0.6 μM) in 50 mM Tris–HCl (pH 7.0) were filtered with Schleicher and Schull Centrex® MF 0.45 μm cellulose acetate sterile centrifugal microfilters upon renaturation and the absorbance at 260 nm

was measured to verify the concentration. Fluorescence of the Y base was measured by exciting $tRNA^{Phe}$ solutions at 318 nm and monitoring the emission at 437 nm. Fluorescence emission spectra were averaged over three scans from 410–460 nm at a scan speed of 400 nm/min. $MgCl_2$, spermine, kanamycin A, and neomycin B (see Fig. 3 for concentrations) were titrated into solution 1 μL at a time to a 2500 μL volume sample (no more than 15 μL total were added to one sample) and fluorescence was measured after a minimum of 10 min incubation with each addition.

Fluorescence studies with EB complexed to $tRNA^{Phe}$ were executed by excitation at 546 nm and following the emission at 598 nm. $tRNA^{Phe}$ (0.2 μM) in 50 mM Tris–HCl (pH 7.0) and 100 mM NaCl was folded both in the presence and absence of 1 mM $MgCl_2$. EB was added to each sample and equilibrated for 30 min at room temperature. Solutions were filtered (as described above) and the absorbance at 260 nm was measured. Fluorescence emission was averaged over three scans from 570 to 700 nm at a scan speed of 400 nm/min. $MgCl_2$, spermine, kanamycin A, neomycin B, and Neo–Neo (see Figure 4 for concentrations) were titrated into solution 1 μL at a time to a 2500 μL volume sample (no more than 10 μL total were added to one sample) and fluorescence was measured after a minimum of 10 min incubation with each addition.

Pb^{2+}-mediated cleavage of $tRNA^{Phe}$

The degree of Pb^{2+}-mediated $tRNA^{Phe}$ cleavage was determined using 5′- or 3′-^{32}P labeled $tRNA^{Phe}$. Neo–Neo (0.025 μM–50 μM), neomycin B (0.01 μM–10 mM), kanamycin A (1 μM–10 mM) or spermine (1 μM–10 mM) were added to individual tubes of folded $tRNA^{Phe}$ (2 μM with trace radiolabeled $tRNA^{Phe}$) in 50 mM Tris–HCl (pH 7.0), 100 mM NaCl, 0.01% Nonidet P-40, and 10 mM $MgCl_2$ and incubated for 1 h. Aliquots of $Pb(OAc)_2$ were added to the final reaction solution (10 μL) at a concentration of 200 μM. After 15 min at room temperature the reaction mixture was quenched with an equal volume of loading buffer (8 M urea, 50 mM EDTA, 0.1×Tris–Borate–EDTA (TBE), 0.14 nM bromophenol blue, and 0.19 nM xylene cyanol FF). The tubes were heated to 75°C for 3 min and loaded on a 15% polyacrylamide/7 M urea gel. Individual bands were quantified using a Phosphorimager and Imagequant™ software. Semilogarithmic plots of the ratio of full-length $tRNA^{Phe}$ to cleavage product versus ligand concentration gave sigmoidal inhibition curves. Each data point x (obtained as a percentage of $tRNA^{Phe}$ cleavage) was normalized to give relative inhibition by calculating $1-[(x-x_{low})/(x_{high}-x_{low})]$. The values for x_{high} and x_{low} correspond to the baseline and the plateau of the sigmoidal curve. The empirical function $f=(x/IC_{50})^n/[1+(x/IC_{50})^n]$ derived from the Hill Equation was applied for curve fitting (x = ligand concentration, n = Hill Coefficient). The concentrations at inflection points yield IC_{50} values. A false point was added in the curve obtained for spermine since full inhibition was never reached at concentrations up to 10 mM.

Gel mobility shift assay

Neo–Neo and neomycin B (see Figure 6 for concentrations) were added to individual tubes of $tRNA^{Phe}$ (2 μM with trace 5′-^{32}P labeled $tRNA^{Phe}$) in 50 mM Tris–acetate (pH 6.8), 20 mM NaCl, 0.01% Nonidet P-40, and 10 mM $MgCl_2$ and incubated for 1 h. Loading buffer (30% glycerol with 0.14 nM bromophenol blue, and 0.19 nM xylene cyanol FF) was added, and samples were loaded on a 12% native polyacrylamide gel and run at room temperature in a 1×running buffer (50 mM Tris–acetate (pH 6.8), 20 mM NaCl, and 10 mM $MgCl_2$).

Aminoglycoside-induced $tRNA^{Phe}$ cleavage

Aminoglycoside-induced cleavage of $tRNA^{Phe}$ has been observed under a variety of conditions including the presence and absence of $MgCl_2$. A representative procedure is outlined below. Neo–Neo (0.025 μM–50 μM) and neomycin B (0.01 μM–10 mM) were added to individual tubes of folded $tRNA^{Phe}$ (2 μM with trace radiolabeled $tRNA^{Phe}$) in 50 mM Tris–HCl (pH 7.0), 100 mM NaCl, 0.01% Nonidet P-40, and 10 mM $MgCl_2$ (10 μL total volume), and incubated for 1 h. An equal volume of loading buffer (8 M urea, 50 mM EDTA, 0.1×TBE, 0.14 nM bromophenol blue, and 0.19 nM xylene cyanol FF) was added to each tube after incubation. The tubes were heated to 75°C for 3 min and loaded on a 15% polyacrylamide/7 M urea gel. Individual bands were quantified using a Phosphorimager and Imagequant™ software.

Enzymatic footprinting of $tRNA^{Phe}$

Neo–Neo (10 μM), neomycin B (100 μM), kanamycin A (1 mM) or spermine (10 mM) were added to individual tubes of folded $tRNA^{Phe}$ (2 μM with trace 5′- or 3′-^{32}P labeled $tRNA^{Phe}$) in 50 mM Tris–HCl (pH 7.0), 100 mM NaCl, 0.01% Nonidet P-40, and 10 mM $MgCl_2$, and incubated for 1 h. RNases were added to a final volume of 10 μL and the solutions were incubated for 20 min at 37°C and then quenched on ice with an equal volume of loading buffer (8 M urea, 50 mM EDTA, 0.1×TBE, 0.14 nM bromophenol blue, and 0.19 nM xylene cyanol FF). The tubes were heated to 75°C for 3 min and loaded on a 15% polyacrylamide/7 M urea gel. Enzymes used include 100 units/μL RNase T1 (cleaves primarily single stranded GpN after the 3′ phosphate), 2.5 units/μL RNase V1 (cleaves indiscriminately double stranded regions after the 3′ hydroxyl group) or 1×10^{-6} units/μL RNase A (cleaves single stranded PypN after the 3′ phosphate).

Fe(II)-EDTA footprinting of $tRNA^{Phe}$

Neo–Neo and neomycin B were added to individual tubes of $tRNA^{Phe}$ (2 μM with trace 5′- or 3′-^{32}P labeled $tRNA^{Phe}$) in 50 mM Tris–HCl (pH 7.0), 100 mM NaCl, 0.01% Nonidet P-40, and 10 mM $MgCl_2$, and incubated for 1 h. Freshly prepared Fe(II)–EDTA and sodium ascorbate/H_2O_2 solutions were then added to give a final concentration of 1 mM Fe(II), 2 mM EDTA,

0.35% H_2O_2, and 1 mM sodium ascorbate in a final reaction volume of 10 μL. Tubes were mixed thoroughly and heated to 37°C for 1 h and quenched with an equal volume of thiourea-containing loading buffer (1 M thiourea, 7 M urea, 50 mM EDTA, 0.1×TBE, 0.14 nM bromophenol blue, and 0.19 nM xylene cyanol FF). The tubes were heated to 75°C for 3 min and loaded on a 15% polyacrylamide/7 M urea gel. Levels of footprinting and enhanced cleavage were normalized by calculating [(intensity of $tRNA^{Phe}$ w/ Neo–Neo)/(intensity of $tRNA^{Phe}$ alone)×100]−100.

Acknowledgements

This research was supported by the National Institutes of Health (grant No. AI 40315) and the University AIDS Research Program, University of California (grant No. R97-SD-036). Special thanks to Andrew Dutton for assistance with the thermal denaturation studies, Chris W. Thomas for help with generating Figure 11, Dr. Katja Michael for insightful discussions, Professor David Kearns for thoughtful discussions along with use of his temperature-controlled UV spectrometer, as well as Dr. Thomas Hermann and Professor Eric Westhof (IBMC-CNRS, Strasbourg) for sharing information prior to publication.

References and Notes

1. Hermann, T.; Westhof, E. *Curr. Opin. Biotech* **1998**, *9*, 66.
2. Pearson, N. D.; Prescott, C. D. *Chem. Biol.* **1997**, *4*, 409.
3. Michael, K.; Tor, Y. *Chem. Eur. J.* **1998**, *4*, 2091.
4. Moazed, D.; Noller, H. F. *Nature* **1987**, *327*, 389.
5. von Ahsen, U.; Davies, J.; Schroeder, R. *Nature* **1991**, *353*, 368.
6. von Ahsen, U.; Davies, J.; Schroeder, R. *J. Mol. Biol.* **1992**, *226*, 935.
7. Davies, J.; von Ahsen, U.; Schroeder, R. In *The RNA World*; Gesteland, R. F., Atkins, J. F., Eds.; Cold Springs Harbor Laboratory: New York, 1993; pp 185–204.
8. Stage, T. K.; Hertel, K. J.; Uhlenbeck, O. C. *RNA* **1995**, *1*, 95.
9. Wang, H.; Tor, Y. J. *Am. Chem. Soc.* **1997**, *119*, 8734.
10. Rogers, J.; Chang, A. H.; von Ahsen, U.; Schroeder, R.; Davies, J. *J. Mol. Biol.* **1996**, *259*, 916.
11. Chia, J.-S.; Wu, H.-L.; Wang, H.-W.; Chen, D.-S.; Chen, P.-J. *J. Biomed. Sci.* **1997**, *4*, 208.
12. Zapp, M. L.; Stern, S.; Green, M. R. *Cell* **1993**, *74*, 969.
13. Mei, H.-Y.; Galan, A. A.; Halim, N. S.; Mack, D. P.; Moreland, D. W.; Sanders, K. B.; Troung, H. N.; Czarnik, A. W. *Bioorg. Med. Chem. Lett.* **1997**, *5*, 2755.
14. Wang, H.; Tor, Y. *Angew. Chem., Int. Ed.* **1998**, *37*, 109.
15. Hermann, T.; Westhof, E. *J. Mol. Biol.* **1998**, *276*, 903.
16. Tor, Y.; Hermann, T.; Westhof, E. *Chem. Biol.* **1998**, *5*, R277.
17. Wallis, M. G.; von Ahsen, U.; Schroeder, R.; Famulok, M. *Chem. Biol.* **1995**, *2*, 543.
18. Lato, S. M.; Boles, A. R.; Ellington, A. D. *Chem. Biol.* **1995**, *2*, 291.
19. Wang, Y.; Rando, R. R. *Chem. Biol.* **1995**, *2*, 281.
20. Jiang, L.; Suri, A. K.; Fiala, R.; Patel, D.J. *Chem. Biol.* **1997**, *4*, 35.
21. Fourmy, D.; Recht, M. I.; Blanchard, S. C.; Puglisi, J. D. *Science* **1996**, *274*, 1367.
22. Recht, M. I.; Fourmy, D.; Blanchard, S. C.; Dahlquist, K. D.; Puglisi, J. D. *J. Mol. Biol.* **1996**, *262*, 421.
23. Jiang, L. C.; Patel, D. J. *Nature Struct. Biol.* **1998**, *5*, 769.
24. Hendrix, M.; Priestley, E. S.; Joyce, G. F.; Wong, C.-H. *J. Am. Chem. Soc.* **1997**, *119*, 3641.
25. Alper, P. B.; Hendrix, M.; Sears, P.; Wong, C.-H. *J. Am. Chem. Soc.* **1998**, *120*, 1965.
26. Wang, Y.; Hamasaki, K.; Rando, R. R. *Biochemistry* **1997**, *36*, 768.
27. Blackburn, G. M.; Gait, M. J. In *Nucleic Acids in Chemistry and Biology,* 2nd Ed.; Oxford University: Oxford, 1996; p 241.
28. Teeter, M. M.; Quigley, G. J.; Rich, A. In *Nucleic Acid–Metal Ion Interactions*; Spiro, T. G., Ed.; Wiley-Interscience: New York, 1980; pp 146–177.
29. Saenger, W. In *Principles of Nucleic Acid Structure*; Springer–Verlag: New York, 1984; pp 331–349.
30. Kim, S. H.; Quigley, G. J.; Suddath, F. C.; McPherson, A.; Sneden, D.; Kim, J.; Rich, A. *Science* **1973**, *179*, 285.
31. Crothers, D. M.; Reid, B. R.; Hurd, R. E.; Johnston, P. D.; Redfield, A. G. In *Transfer RNA: Structure, Properties, and Recognition*; Schimmel, P. R., Söll, D., Abelson, J. N., Eds.; Cold Springs Harbor Laboratory: New York, 1979; pp 163–206.
32. Quigley, G.; Teeter, M.; Rich, A. *Proc. Natl. Acad. Sci. USA* **1978**, *75*, 64.
33. Loftfield, R. B.; Eigner, A. E.; Pastuszyn, A. *In Polyamines in Biology and Medicine*; Morris, D. R., Marton, L. J., Eds.; Marcel Dekker: New York, 1981; pp 207–221.
34. Brown, R. S.; Dewan, J. C.; Klug, A. *Biochemistry* **1985**, *24*, 4785.
35. Jack, A.; Ladner, J. E.; Rhodes, D.; Brown, R. S.; Klug, A. *J. Mol. Biol.* **1977**, *111*, 315.
36. Frydmann, B.; Westler, W. M.; Samejima, K. *J. Org. Chem.* **1996**, *61*, 2588.
37. Botto, R. E.; Coxon, B. *J. Am. Chem. Soc.* **1983**, *105*, 1021.
38. Wang, H.; Tor, Y. *Bioorg. Med. Chem. Lett.* **1997**, *7*, 1951.
39. Michael, K.; Wang, H.; Tor, Y. *Bioorg. Med. Chem.* **1999**, *7*, 1631.
40. Denaturation studies in the presence of Neo–Neo (10 μM) are not shown because irregular melting curves were obtained, most likely due to aggregation.
41. Titration of Neo–Neo into a solution of $tRNA^{Phe}$ (0.2 μM) could only be preformed at low concentration (< 10 μM). At higher Neo–Neo concentrations, aggregates are formed.
42. Dock-Bregeon, A. A.; Moras, D. In *Cold Spring Harbor Symposia on Quantitative Biology*; Cold Spring Harbor Laboratory: New York, 1987; Volume LII, pp 113–121.
43. Latham, J. A.; Cech, T. R. *Science* **1989**, *245*, 276.
44. Celander, D. W.; Cech, T. R. *Biochemistry* **1990**, *29*, 1355.
45. Sampson, J. R.; Uhlenbeck, O. C. *Proc. Natl. Acad. Sci. USA* **1988**, *85*, 1033.
46. Eisenberg, D.; Crothers, D. In *Physical Chemistry with Applications to the Life Sciences*; Eisenberg, D., Crothers, D., Eds.; The Benjamin/Cummings Publishing: Menlo Park, CA, 1979; pp 160–162.
47. Takeda, Y.; Samejima, K.; Nagano, K.; Watanabe, M.; Sugeta, H.; Kyogoku, Y. *Eur. J. Biochem.* **1983**, *130*, 383.
48. Szilágyi, L.; Pusztahelyi, Z. S.; Jakab, S.; Kovács, I. *Carbohydr. Res.* **1993**, *247*, 99.
49. Bearley, K.; Tao, T.; Cantor, C. R. *Biochemistry* **1970**, *9*, 3524.
50. Robison, B.; Zimmerman, T. P. *J. Biol. Chem.* **1971**, *246*, 110.
51. Preliminary CD studies suggest a conformational change upon addition of aminoglycosides.
52. Delcros, J-G.; Sturkenboom, M. C.; Baso, H. S.; Shafer, R. H.; Szöllösi, J.; Feuerstein, B. G.; Marton, L. J. *Biochem. J.* **1993**, *291*, 269.

53. Sakai, T. T.; Torget, R.; I, J.; Freda, C.; Cohen, S. *Nucleic Acids Res*. **1975**, *2*, 1005.
54. Jones, C. R.; Bolton, P. H.; Kearns, D. R. *Biochemistry* **1978**, *17*, 601.
55. Brown, R. S.; Hingerty, B. E.; Dewan, J. C.; Klug, A. *Nature* **1983**, *303*, 543.
56. Michalowski, D.; Wrzesinski, J.; Krzyzosiak, W. *Biochemistry* **1996**, *35*, 10727.
57. Behlen, L. S.; Sampson, J. R.; DiRenzo, A. B.; Uhlenbeck, O. C. *Biochemistry* **1990**, *29*, 2515.
58. Krzyzosiak, W. J.; Marciniec, T.; Wiewiorowski, M.; Romby, P.; Ebel, J. P.; Giege, R. *Biochemistry* **1988**, *27*, 5771.
59. Wallace, S.; Schroeder, R. *RNA* **1998**, *4*, 112.
60. Labuda, D.; Nicogrusian, K.; Cedergren, R. *J. Biol. Chem*. **1985**, *260*, 1103.
61. Using a gel mobility shift assay, Mei and co-workers were unable to determine rate constants for neomycin B-TAR complex formation due to a rapid equilibrium between complex and free RNA.[65]
62. Aminoglycoside-induced cleavage occurs under a variety of conditions. It is therefore unlikely that it is induced by RNases, although enhanced susceptibility of tRNA to trace RNases cannot be excluded.
63. Kirk, S. R.; Tor, Y. *Chem. Commun*. **1998**, 147.
64. Chen, Q.; Shafer, R. H.; Kuntz, I. D. *Biochemistry* **1997**, *36*, 11402.
65. Wang, S.; Huber, P. W.; Cui, M.; Czarnik, A. W.; Mei, H.-Y. *Biochemistry* **1998**, *37*, 5549.
66. Robinson, H.; Wang, A. H.-J. *Nucleic Acids Res*. **1996**, *24*, 676.
67. Lavery, R.; Pullman, B. *Nucleic Acids Res*. **1981**, *9*, 4677.
68. Lavery, R.; Pullman, B. *Nucleic Acids Res*. **1982**, *10*, 4383.
69. Hermann, T.; Westhof, E. personal communication.
70. Sambrook, J.; Fritsch, E. F.; Maniatis, T. In *Molecular Cloning* 2nd ed.; Cold Springs Harbor Laboratory: New York, 1989.
71. Bruce, A. G.; Uhlenbeck, O. C. *Nucleic Acids Res*. **1978**, *5*, 3665.